Eur. Phys. J. D **10**, 105–114 (2000)

THE EUROPEAN PHYSICAL JOURNAL D

EDP Sciences

Ab initio molecular dynamics study on Ag_n (n = 4, 5, 6)

Z.F. Liu[1,a], W.L. Yim[1], J.S. Tse[2], and J. Hafner[3]

[1] Department of Chemistry, The Chinese University of Hong Kong, Shatin, Hong Kong, P.R. China
[2] Steacie Institute for Molecular Sciences, National Research Council of Canada, Ottawa, Ontario K1A 0R6, Canada
[3] Institut für Theoretische Physik, Technische Universität Wien, Vienna, Austria

Received 5 May 1999 and Received in final form 20 August 1999

Abstract. *Ab initio* Molecular Dynamics (MD) method, based on density functional theory (DFT) with planewaves and pseudopotentials, was used to study the stability and internal motion in silver cluster Ag_n, with $n = 4-6$. Calculations on the neutral, cationic and anionic silver dimer Ag_2 show that the bond distance and vibrational frequency calculated by DFT are of good quality. Simulations of Ag_4, Ag_5, and Ag_6 in canonical ensemble reveal distinct characteristics and isomerization paths for each cluster. At a temperature of 800 K, an Ag_4 has no definite structure due to internal motion, while for Ag_5 and Ag_6 the clusters maintain the planar structure, with atomic rearrangement observed for Ag_5 but not for Ag_6. At a temperature of 200 K, Ag_4 can exist in two planar structures whilst Ag_5 is found to be stable only in the planar form. In contrast Ag_6 is stable in both planar trigonal and 3D pentagonal structures. Microcanonical MD simulation was performed for all three clusters to obtain the vibrational density of states (DOS).

PACS. 36.40.-c Atomic and molecular clusters – 31.15.Qg Molecular dynamics and other numerical methods – 31.15.Ar Ab initio calculations

1 Introduction

The electronic structure of small metal clusters has long been a subject of intensive theoretical and experimental studies, because of its importance for the understanding of metal-metal interactions, and in catalysis and photography [1–3]. Understanding the geometrical structure of these clusters is more challenging, since for each cluster there are often several possible isomers connected by a flat potential surface and thus the cluster does not have fixed structures due to isomerization and pseudorotation. The dynamics of such processes in small metal clusters as a function of temperature, first studied by classical molecular dynamics (MD) method, revealed interesting solid-liquid and liquid-gas-like transformations [4,5], although designing an accurate empirical potential surface for these clusters is non-trivial. Recent development of *ab initio* molecular dynamics [6–12] offered a powerful new method to study such structural transformation, as the electronic energy and ionic force are calculated from first principle at either Hartree-Fock [13,14], local density approximation [15,16], or even post Hartree-Fock levels [17]. Alkali metal clusters, such as sodium [15,16] and lithium clusters [13,14,17], have received most attention, since these systems are among the simplest with each metal atom contributing only one valence electron. The experimental progress in the high resolution spectroscopic measurement of metal clusters [18,19], and especially the development of femtosecond laser system coupled with a negative ion-neutral-positive ion charge reversal apparatus which offers time resolved direct probe at the dynamics of the internal motion [20–22], are likely to provide further impetus for such theoretical efforts, especially for small clusters with $n = 3-6$.

Among transition metal clusters, silver clusters have received considerable attention from both experimentalists [18,19,21–29] and theoreticians [31–46]. In terms of electronic structure, transition metal clusters are more complicated than alkali metal clusters because of the presence of d electrons. However, a silver atom has a completely filled $4d$-shell and one $5s$ valence electron, and silver clusters are often thought to be analogous to alkali metal clusters in terms of electronic configuration [33]. To date, the most detailed study on the Ag_n clusters used an effective core potential for the $4d$ shell and configuration interaction method to account for the correlation effects which were always important in transition metal species [31]. In addition, there is an extensive theoretical literature on the geometrical structures of Ag_n clusters at various accuracy levels [34–43]. Although these calculations may differ in their prediction of the most stable structure for some clusters (for example, Ag_5 and Ag_6 [31,34,40]), depending on the level of theoretical treatment and whether d electrons are included in the calculation, they agreed with each other in that each cluster

[a] e-mail: zfliu@cuhk.edu.hk

of a certain size ($n = 3-9$) was found to have several geometrical isomers which were close in energy, implying interesting vibrational dynamics for these clusters at constant temperature.

Classical molecular dynamics simulations have been performed very recently to study the dynamics of Ag_6, using a potential surface fitted to points in configuration space calculated by density functional theory [44–46]. The presence of d electrons has made *ab initio* MD simulations on silver clusters computationally much more demanding than simulations for alkali metal clusters. To our best knowledge no such studies have been reported in the literature except for Hartke and Carter's *ab initio* MD study on Ni_5 cluster in which the d electrons were frozen [47]. Studies on the alkali metal cluster have focussed on clusters with a size larger than 8 [13–16], except for the recent study by Gibson and Carter on Li_5 [17].

In this article, we report an *ab initio* MD study on the dynamics of Ag_n, with $n = 4-6$, taking advantage of the recent development of the spin-polarized non-local density method and of ultrasoft pseudopotentials [9–12]. After a careful study on neutral, cationic and anionic silver dimer to verify the quality of our method, we will explore the dynamics of the internal motion for Ag_4, Ag_5, and Ag_6, at temperatures ranging from 200 to 800 K, to see its dependence both on the cluster size and on temperature.

2 Computational method

The principles of *ab initio* MD method based on total energy calculation by density functional theory with a planewave basis set and pseudopotentials have been documented in the literature [6–8]. The *ab initio* total energy and molecular dynamics program VASP (Vienna *ab initio* simulation program) was used in the present study [9–12]. A silver cluster is put in a large cubic box to imitate gas phase conditions. The lattice parameter is 12 Å for silver tetramer, and 15 Å for dimer, pentamer and hexamer.

Ultrasoft pseudopotential for silver atom with the Ceperly-Alder type local exchange correlation functional [48], and with/without the Perdew-Wang [49] type generalized gradient correction (GGA), was used in the calculation. The silver potential was generated with a reference configuration of $d^{10}s^1$ and based on scalar relativistic wavefunctions with relativistic core-effects taken into account. Extensive tests on such potentials showed a significant reduction in the planewave cutoff energy [50], and for our simulation the cutoff energy was 180 eV. Unless specified otherwise, the spin-restricted method was used for closed shell clusters and the spin-unrestricted for open shell clusters. The optimization for total electronic energy was performed by conjugate gradient method, and cluster structures reported by Bonačić-Koutecký *et al.* [31] were used as the starting point for geometrical optimization.

To investigate the thermal stability of Ag_n, $n = 4-6$, molecular dynamics (MD) calculations in the canonical ensemble with a Nosé-Hoover thermostat [51] were performed. Time step used in the MD simulations was 2 fs. Atomic Equivalence Index (AEI) as defined in reference [14] is a very sensitive order parameter to monitor structural changes and is used in the analysis of the trajectories. For the ith atom, AEI(σ) is given as,

$$\sigma_i = \sum_{j \neq i}^{n} |\mathbf{r}_i - \mathbf{r}_j| \tag{1}$$

and the summation is over all distances from atom i to all other atoms within the cluster. In addition, the root-mean-square bond length fluctuations, δ,

$$\delta = \frac{2}{n(n-1)} \sum_{i<j}^{n} \frac{[\langle r_{ij}^2 \rangle - \langle r_{ij} \rangle^2]^{1/2}}{\langle r_{ij} \rangle} \tag{2}$$

is also calculated to measure thermal stability and to be compared with previous MD simulations on Ag_6 [44].

Micro-canonical MD simulations were also performed on selected isomers for Ag_4, Ag_5, and Ag_6. The time step used was again 2 fs, and total duration was 10 ps (5000 steps). The atom velocity correlation function and its Fourier transform was then calculated. When the simulation duration is varied, peak positions change very little, while peak widths change slightly. The peak height so obtained is proportional to the density of states, rather than the experimental IR intensity.

3 Results and discussion

3.1 Ag_2

Ag_2 is the simplest and most studied silver cluster, therefore a good model to test the quality and accuracy of our computational procedure. We conducted a detailed study on the neutral silver dimer and its cation and anion. For each species, about 40 points on the potential surface were calculated with internuclear distance ranging from 1.8 to 4.0 Å. These points were numerically fitted to a Morse potential to extract the equilibrium bond distance and vibrational frequency. The dissociation energy was calculated from the energy difference between the dimer and the corresponding isolated atom/ion. Four different levels of approximation were used in the calculation: local density approximation (LDA), spin-polarized LDA (LSDA), Perdew-Wang gradient corrections (GGA) [49], and spin-polarized GGA. The results obtained here are compared with previous experimental and theoretical studies in Tables 1 and 2.

In general, the calculated bond distances and vibrational frequencies are in good agreement with previous experimental and theoretical results. The dissociation energy is often overestimated, but GGA and spin-polarization improve the results. GGA are used for all subsequent simulations. For closed-shell Ag_4 and Ag_6, spin-restricted calculation is performed. In the early days of the application of the *ab initio* molecular dynamics method to metal clusters, spin-restricted method was often employed even for open-shell systems. To examine the validity of this simplification, both spin-polarization and spin-restricted methods are attempted for the open-shell Ag_5 cluster.

Table 1. Comparison of the calculated and experimental ground state properties of Ag_2 dimer.

	Method	R_e (Å)	ω_e (cm^{-1})	D_e (eV)	Ref.
Ag_2	LDA	2.497	203.1	2.577	---
	LSDA	2.497	203.2	2.274	---
	LDA + GGA	2.574	182.3	2.149	---
	LSDA + GGA	2.574	182.3	1.784	---
	CI-1*e*-RECP-CVC, (4*s*4*p*) AO basis set contracted to (211/211)	2.628	181.0	1.595	1
	CI-1*e*-RECP-CVC, α_d=0.200	2.620	187.3	1.683	1
	CI-1*e*-RECP-CVC, α_d=0.020	2.628	180.9	1.598	1
	CI-1*e*-RECP-CVC, α_{s1}=0.01, α_{s2}=0.003, α_p=0.003	2.627	180.8	1.595	1
	Exp.	2.530	192.4	1.65	23,24

Table 2. Comparison of the calculated and experimental ground state properties of Ag_2^+ and Ag_2^- dimer.

	Method	R_e (Å)	ω_e (cm^{-1})	D_e (eV)	Ref.
Ag_2^+	LSDA	2.609	155.6	2.199	---
	LSDA + GGA	2.730	129.7	1.870	---
	LDA + GGA	2.735	128.1	1.921	---
	CI-1*e*-RECP-CVC, (4*s*4*p*) AO basis set contracted to (211/211)	2.850	128.2	1.648	1
	Exp.	2.625	135.8	1.570	22
Ag_2^-	LSDA	2.597	159.1	1.750	---
	LSDA + GGA	2.709	133.6	1.370	---
	LDA + GGA	2.718	130.7	1.426	---
	CI-1*e*-RECP-CVC, (4*s*4*p*) AO basis set contracted to (211/211)	2.776			30
	Exp.	2.655	145.0	1.37	18

3.2 Ag_4

The rhombic structure is found to be the most stable Ag_4 isomer, and the planar isomer 0.21 eV higher in energy (Fig. 1). This is consistent with previous studies, which found an energy difference of 0.20 eV by all-electron spin-density calculations [34] and 0.61 eV by RECP method [31].

An analysis of the AEI shows that the Ag atoms in the D_{2h} Ag_4 rhombic cluster can be divided into two groups,

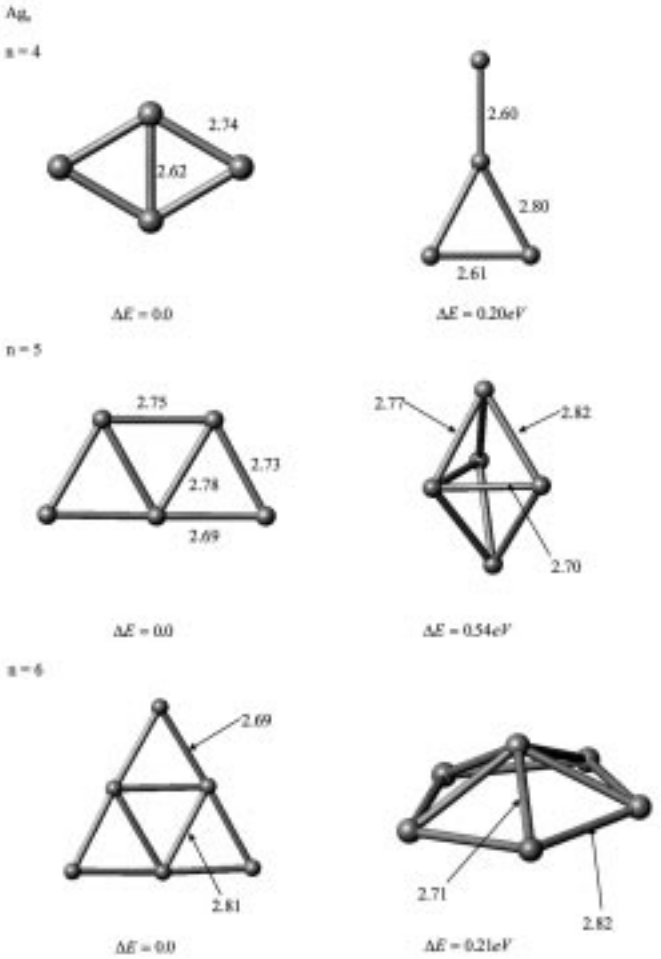

Fig. 1. The two lowest energy isomers for Ag_4, Ag_5, and Ag_6. ΔE indicates the relative energy to the most stable isomer, based on LDA/LSDA calculations.

as in Figure 2. Below 600 K, the distinction between these two groups of atoms is maintained throughout the entire duration of the 10 ps simulation. As the temperature is raised from 200 K to 600 K, the δ value defined in (2) increases from 0.031 to 0.045 as shown in Table 3, indicating larger fluctuations. There is no abrupt change in the indices and no crossing between the two groups, as the cluster maintains the rhombic structure. The Ag_4 structure changes dramatically at 800 K when large fluctuations in the AEI index and many crossings are observed. The Ag atoms in the cluster execute continuous internal motions without any definite shape, and correspondingly δ value jumps four times from 600 K to 800 K.

Although planar Ag_4 is less stable than the rhombic structure, a dynamical simulation shows that the planar cluster is metastable at 200 K (Fig. 2c). In a planar Ag_4, the Ag atoms fall into three categories, and Figure 2c exhibits an interesting and regular pattern, which can be attributed to the sidewise waggling of atom 2.

When the temperature is raised from 200 K to 400 and 600 K, the planar structure isomerizes to the rhombic

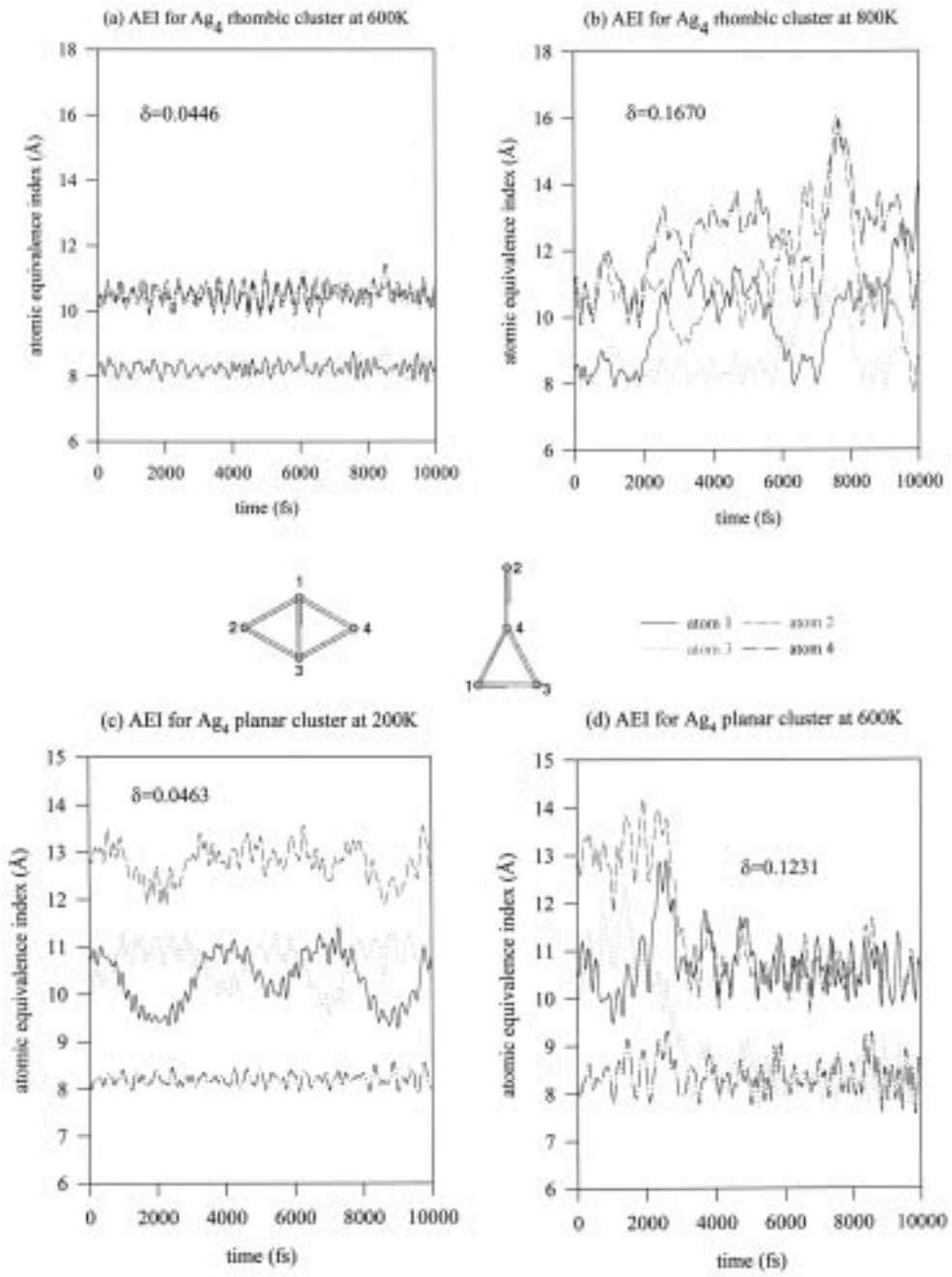

Fig. 2. The AEI plots for rhombic Ag_4 at 200 and 800 K, and for planar Ag_4 at 200 and 600 K.

structure, with corresponding crossings in the AEI shown in Figure 2d. The δ value of 0.046 for planar Ag_4 at 200 K is larger than the δ value of 0.031 for rhombic Ag_4 (Tab. 3). The large increase in the δ values from 200 K to 400 and 600 K, is associated with the isomerization process. At 800 K, the AEI is again quite irregular and a δ value of 0.17 indicates significant increase in the extent of internal motion.

The isomerization path from the planar to the rhombic structure can be rationalized by an inspection of the symmetry of the frontier orbitals. Since the isomerization is a thermally activated process, the orbital symmetry must be conserved throughout the reaction pathway. As shown in Figure 3, which is generated by a simple extended Hückel calculation, the interaction between the Ag atoms in the base of the triangle and the apical Ag atom is largely antibonding. Therefore, the breaking of the Ag(1)–Ag(3) or Ag(2)–Ag(3) bond is most facile. The cleavage of the Ag–Ag bond is followed by rehybridization of Ag(2). Eventually, the in-phase interactions between Ag(1)–Ag(2) and between Ag(1)–Ag(3) help to stabilize the rhombic structure.

Figure 4 shows the vibrational density of states obtained for rhombic and planar clusters. For both clusters

Table 3. Delta values for silver clusters, Ag_n ($n = 4, 5, 6$). The calculations were performed using LDA+GGA when not mentioned.

	Temperature (K)	δ
Ag_4 rhombic cluster	200	0.031
	400	0.041
	600	0.045
	800	0.167
Ag_4 planar cluster	200	0.046
	400	0.106
	600	0.123
	800	0.170
Ag_5 trapezoidal cluster	200[a]	0.022
	200	0.020
	400[a]	0.085
	800[a]	0.091
Ag_6 planar cluster	400	0.039
	800	0.050
	1500	0.104
	2000	0.365
Ag_6 3D pentagonal cluster	400	0.032
	800	0.094
	1500	0.167
	2000	0.380

a: LSDA+GGA calculation

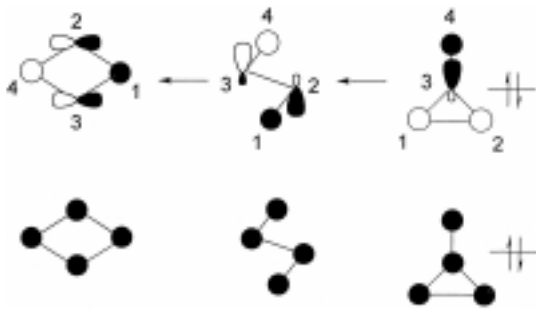

Fig. 3. The symmetry of the two highest occupied molecular orbitals in Ag_4 along the isomerization path.

the vibrational band with the highest frequency is between 150–200 cm^{-1} which can be assigned to the Ag–Ag stretching. The band extending from 70 to 110 cm^{-1} is associated with the bending vibrations. Other lower energy bands can be attributed to torsional motions and pseudorotation at finite temperature. Poteau *et al.* [33] has calculated the harmonic frequencies for the rhombic Ag_4 cluster, which are also indicated in Figure 4. While there is general correspondence between the bands in our DOS plot and the peaks reported by Poteau *et al.*, the discrepancy in frequency could go as high as 20 cm^{-1}.

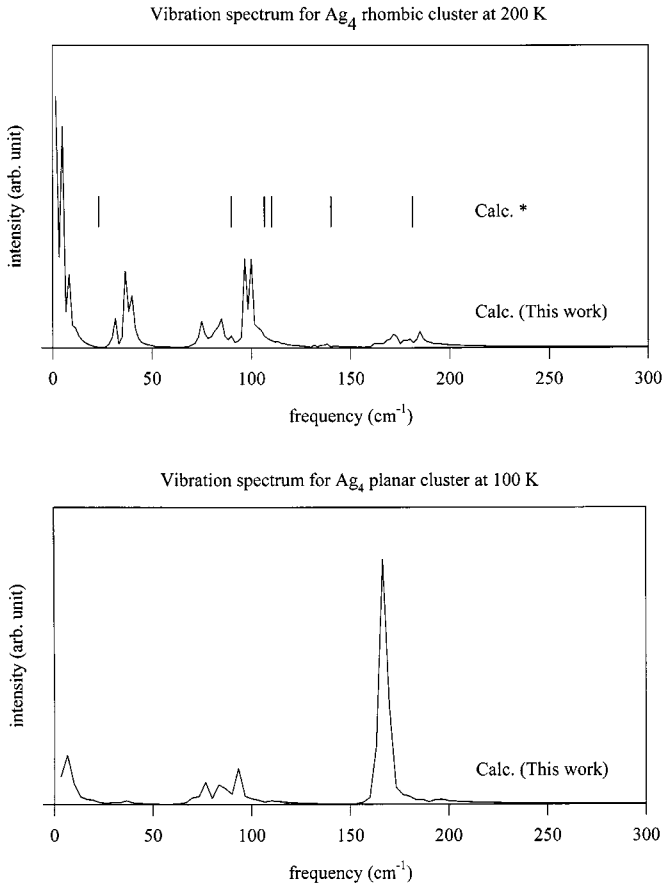

Fig. 4. Vibrational density of state plot for Ag_4 obtained from FFT of velocity autocorrelation function in a 10 ps microcanonical MD simulation: top for rhombic Ag_4 cluster at 200 K; bottom for planar Ag_4 cluster at 100 K. Calculated frequencies (*) for the rhombic Ag_4 are from reference [33].

3.3 Ag_5

The two most stable structures for Ag_5 cluster are the planar trapezoidal and the bipyramidal forms as shown in Figure 1. Theoretical calculations varied in their predictions of the relative stability of the two isomers. Bonačič-Koutecký and co-workers, using the Hartree-Fock method with RECP and configuration interactions (CI) [31] found the two isomers are essentially degenerate with the bipyramidal isomer being more stable by only 0.003 eV. In contrast, also using similar *ab initio* RECP approach, Bauschlicher *et al.* found that the planar isomer was more stable by 0.31 eV [40]. The latter result is further supported by more recent LSDA calculations by Santamaria *et al.* who found an energy difference of 0.47 eV [34]. A similar near degeneracy in the trapezoidal and bipyramidal forms was also noted in a recent *ab initio* calculation on Li_5 [17]. The most stable structure identified is once again the planar trapezoidal. The energy difference between the planar and bipyramidal structures was found to be 0.51 eV at the (Complete Active Space) CASSCF level and only 0.07 eV with multireference double configuration interaction (MRCI) treatment. The present

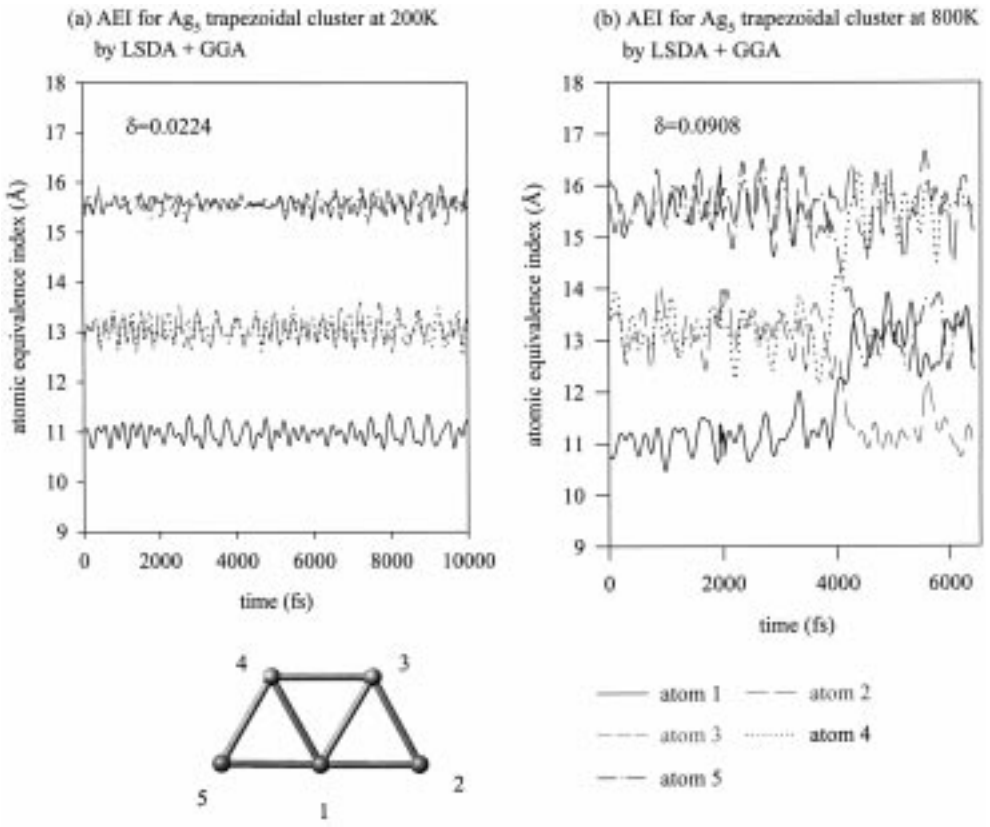

Fig. 5. The AEI plots for Ag_5 at 200 and 800 K, calculated by LSDA+GGA.

result for Ag_5 of 0.53 eV is in agreement with that of Santamaria *et al.* [34], and also in good accord with a very recent Raman measurement on Ag_5 isolated in argon matrix which concluded that Ag_5 should be a planar trapezoidal molecule [18].

MD simulations of Ag_5 with Nosé thermostat at 200, 400 and 800 K were performed with LSDA calculations. The duration of the simulation was 6 ps. According to the AEI, the silver atoms in planar trapezoidal Ag_5 could be divided into three categories as shown in Figure 5. The structure is stable at 200 K. At 400 K and 800 K, the planar structure is preserved during the entire simulation time of 6 ps, but the trajectories show crossing of the AEI lines indicating rearrangement of atoms within the cluster, but the overall structure is unchanged. The pathway is shown schematically in Figure 6. Compared to the rhombic Ag_4 cluster, Ag_5 is obviously more mobile at 400 K. On the other hand, it is noteworthy that raising the temperature to 800 K does not result in any significant increase in the δ (Tab. 3) value and the AEI does not show any irregular pattern.

MD simulations of the bipyramidal Ag_5 at 50 and 200 K, starting from the equilibrium structure, were also attempted. In both cases, the bipyramid isomerized into the planar form within less than 1 ps. The bottom of Figure 6 shows a typical isomerization path observed. This behavior was in agreement with Gibson and Carter's recent simulation on Li_5 [17], and provided further support to the experimental conclusion based on Raman measurement that Ag_5 exists only in the planar form in the matrix [18].

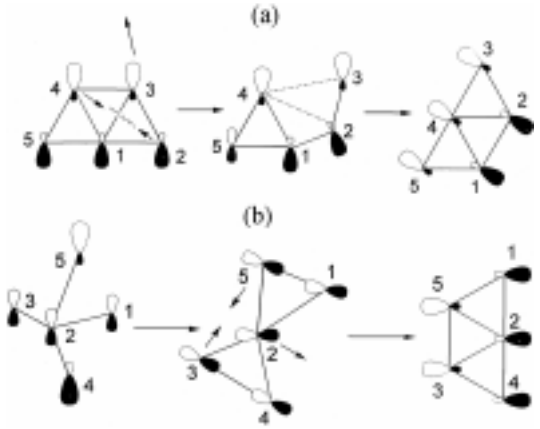

Fig. 6. The orbital symmetry of the SOMO in Ag_5 along the atomic rearrangement path for planar Ag_5 (a) and along the isomerization path from the bipyramidal to the planar structure (b).

During the atomic rearrangement, the symmetry of the singly occupied molecular orbital (SOMO) in planar Ag_5 is conserved. Figure 6, generated again by extended Hückel calculation along the transformation path, shows that the preferential breaking of the Ag(1)–Ag(3) (or Ag(1)–Ag(4)) bond is due to a slight antibonding character of the bond.

After the cleavage of the 1, 3 bond, Ag(2) moves closer to Ag(4), while Ag(5) atom rehybridizes, leading to an increased positive lobe (in white color) and enhancing the bonding interaction with Ag(4). The isomerization pathway from the bipyramidal to the planar structure can also be rationalized similarly by the SOMO symmetry. Starting from the bipyramidal structure, the interaction between Ag(1)–Ag(5) and Ag(3)–Ag(4) are conserved, but the bonding between Ag(3)–Ag(5) and among Ag(1), Ag(2) and Ag(4) are greatly strengthened after the isomerization.

Figure 7a shows the vibrational density of state plots obtained for Ag_5, which can be compared with both the recent experimental Raman spectrum [18] and previous DFT calculation [33]. The strong band around 150 cm^{-1} and the weak band around 180 cm^{-1} should be compared with the Raman peaks at 162 cm^{-1} and 174 cm^{-1}. However, one should keep in mind that the peak height in a DOS plot is not directly comparable to the experimental intensity. Overall in the frequency region above 50 cm^{-1}, there are reasonable correspondences between the experimental observation and our calculations.

To investigate the importance of spin polarization effect on the dynamics for an open-shell cluster as Ag_5, MD simulations for Ag_5 at 200 K were performed in both the spin-restricted (LDA) and spin-polarized approximations (LSDA). The evolution of AEI and the Fourier transform of the atomic velocity autocorrelation function for these two cases are very similar to each other, even though two different approaches were employed.

3.4 Ag_6

Ag_6 has been studied previously by both *ab initio* RECP method and all-electron spin density method. The *ab initio* RECP method at Hartree-Fock level [31] found the two isomers illustrated in Figure 1 and an additional tripyramidal structure all lying within 0.06 eV in energy. Post Hartree-Fock CI treatment raised the energy of the planar trigonal isomer to be the highest among the three and 0.27 eV higher than the most stable pentagonal isomer. However, the CI treatment in the reported results [31] was based on the SCF optimized structures and no further geometrical optimization was performed at the CI level. Such optimization could be quite important when the energy difference between these isomers were small. Independently, Liao and Balasubramanian [43] performed geometry optimization at the CASSCF and CI level, using *ab initio* RECP method, but unfortunately they did not include the planar trigonal isomer into consideration. Santamaria *et al.* optimized these structures using the all-electron LSDA [34] and found the planar trigonal isomer to be the most stable structure with the pentagonal pyramid structure only 0.15 eV above it. The present result is again in good agreement with Santamaria *et al.*'s calculations and the energy difference between the trigonal and the pentagonal structures is 0.21 eV. Due to limitation of computational resource, *ab initio* MD simulations were performed for the trigonal and pentagonal isomers only. The tripyramidal structure, which was 0.58 eV higher in energy than the trigonal structure according to Santamaria *et al.*'s results [34], was not considered.

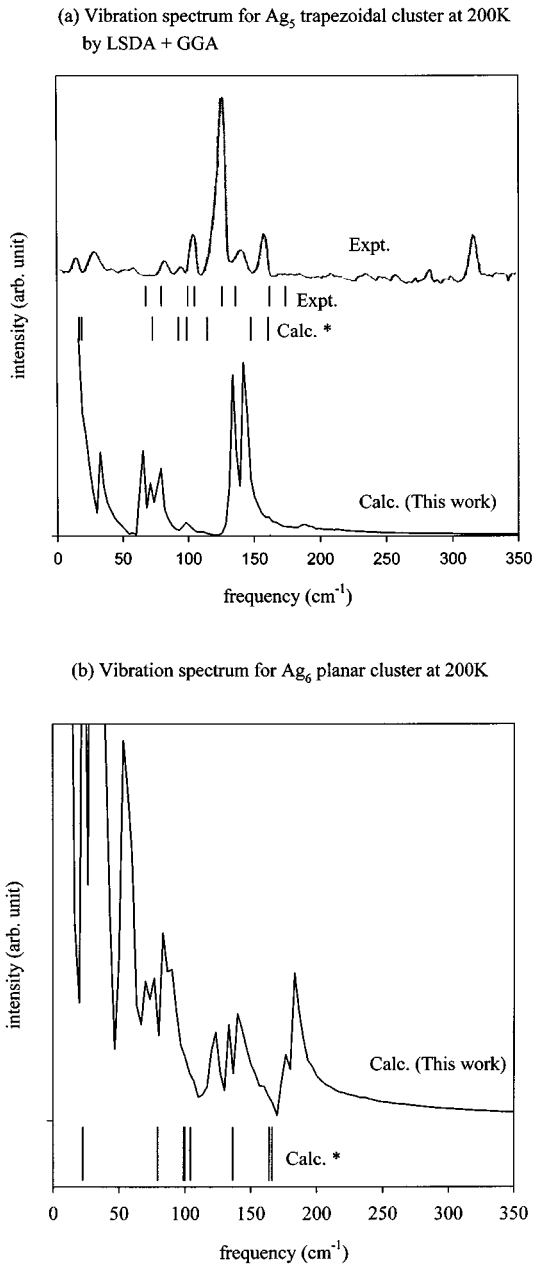

Fig. 7. (a) Vibrational density of state plot for planar Ag_5, together with the previous experimental spectrum from reference [18]. (b) Vibrational DOS plot for planar Ag_6. Calculated frequencies (*) labeled by vertical bars are from reference [33].

Starting from the triangular shape of Ag_6, the AEI of the six Ag atoms fall into two categories. The first group consists of the three Ag atoms at the corners and the other group of the three Ag atoms at the mid-points of the sides. It is a natural growth from the Ag_5 planar isomer with an Ag atom added to transform the W-shaped planar Ag_5 into a triangle which is remarkably stable upon heating. At 400 and 800 K, the two classes of AEI in Figure 8

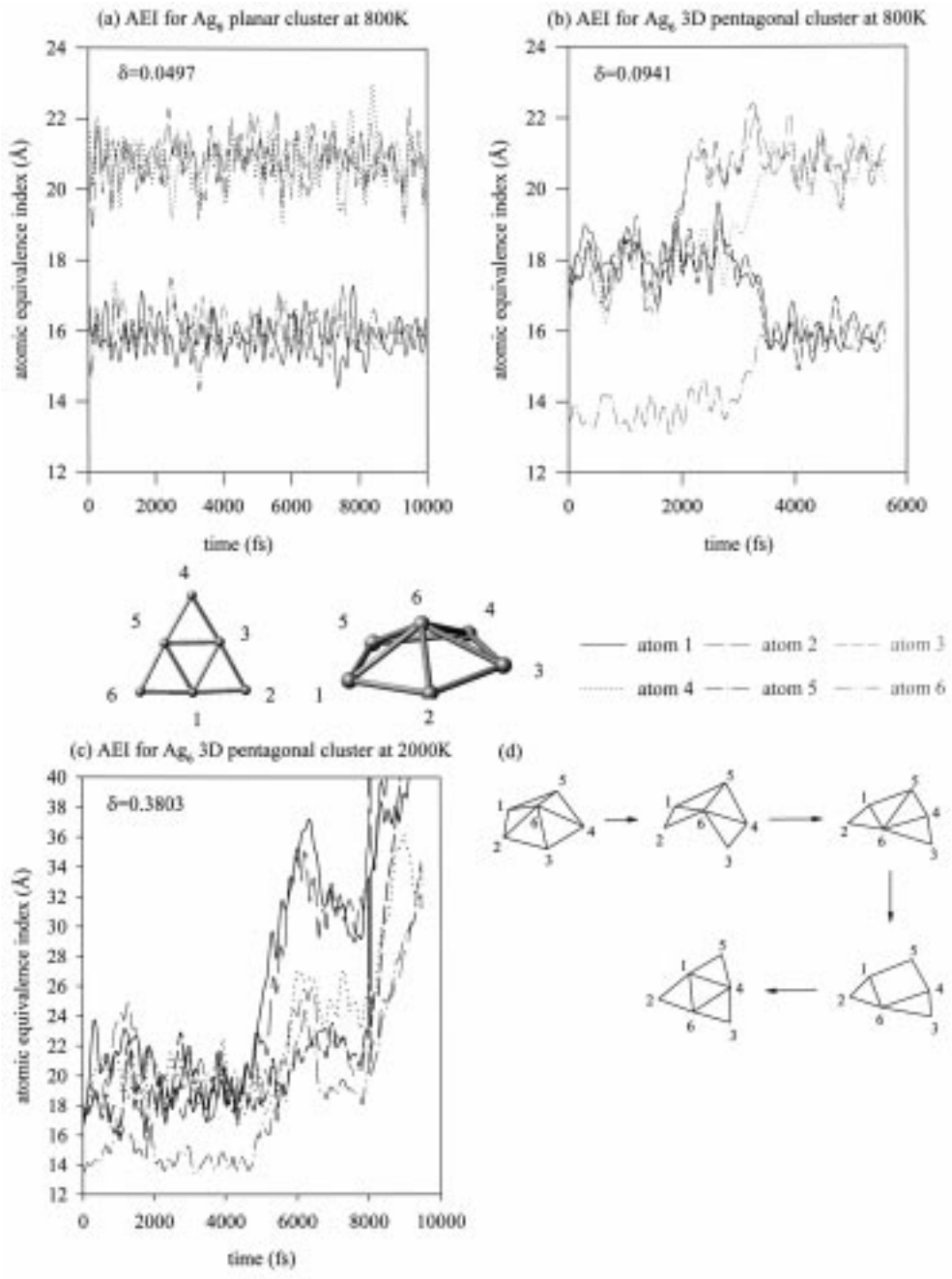

Fig. 8. The AEI plots for the planar Ag_6 at 800 and 2000 K (a, b), and for the pentagonal Ag_6 at 800 K (c), and the isomerization path from the pentagonal to the planar structure (d).

did not cross, and Ag_6 always maintained a rigid planar triangular structure. The δ value of 0.050 (Tab. 3) for Ag_6 at 800 K is considerably smaller than the δ values for Ag_4 and Ag_5 at the same temperature.

The second Ag_6 isomer, the pentagonal structure, is also fairly rigid. At 400 K, the cluster maintained its pentagonal structure for the entire duration of 10 ps simulation. Even at 800 K, the pentagonal structure survived more than 4 ps before isomerizing into the planar form, and the observed transformation pathway is shown in Figure 8d. It indicates that although the 2D planar structure is still the most stable, the 3D Ag_6 structure is much more stable than its Ag_5 cousins. With Ag_7 definitely taking the 3D form [27], Ag_6 could be considered as an intermediate case within the general trend of transition from 2D to 3D structures as the number of atoms increased in a metal cluster.

Classical MD simulations [44–46] on these isomers were reported recently based on a potential surface fitted to DFT calculations. As discussed above, the structures and energetics for Ag_5 and Ag_6 obtained by these DFT calculations [34] are in very good agreement with our results.

Ab initio MD method treats the nuclear motion in the same way as in the classical MD, both within Newtonian mechanics, and "classical" here refers to the fact that a fitted empirical potential is used. However, our *ab initio* MD results are significantly different from the classical MD results regarding the stability of Ag_6 clusters. Classical MD showed that the planar Ag_6 went through isomerization between 2D and 3D structures at 300 K. Above 500 K such changes speeded up significantly and the cluster was in a "liquidlike phase" [44], and correspondingly the δ value jumped up from 0.05 to 0.3 as the temperature was raised from 300 K to 1000 K. Although we saw similar liquidlike behavior for Ag_4 at 800 K, the Ag_6 clusters are remarkably stable in our *ab initio* MD simulation, especially for the trigonal isomer.

To further study the stability of Ag_6 clusters, simulations at 1500 K and 2000 K are performed for both isomers. Extensive changes between 2D and 3D structures are observed at both temperatures. At 2000 K, our δ values above 0.35 are comparable to the classical MD results at similar temperatures, and fragmentation are also observed for both isomers, in agreement with classical MD [44]. At 1500 K, our δ values (0.10 for trigonal isomer and 0.17 for pentagonal isomer) are about half of the classical MD values. The difference between *ab initio* MD and classical MD results is unlikely due to the length of simulation time. At 400 K, classical MD obtained a δ value around 0.1 [44], close to the corresponding *ab initio* MD value at 1500 K. At 800 K the classical MD δ value is at 0.3, indicating a cluster in a liquidlike state with fast internal motion. If these were indeed true, we should have been able to observe such internal motions at both 400 K and 800 K in *ab initio* simulations. The more likely explanation for the discrepancy between *ab initio* and classical MD results is the quality of the analytical fit for the empirical potential energy surface used in the classical MD simulation.

Figure 7b shows the vibrational DOS plot for Ag_6. The DOS peaks become more congested as the number of modes increases with the number of atoms, and direct comparison with previous calculation are more difficult [33]. Its general features are similar to the DOS of Ag_5 planar cluster in Figure 7a with three group of bands, one just below 200 cm^{-1}, one close to 150 cm^{-1}, and one between 50 and 100 cm^{-1}, although the relative heights of these bands are quite different.

3.5 Summary

Comparison with previous experimental and theoretical calculations on neutral, cationic and anionic Ag_2 dimer showed that planewave/pseudopotential based density functional theory offered a very good description for the Ag–Ag bond distance and stretching vibrational frequency, and thus DFT based *ab initio* MD method should be ideal for the study of the dynamics of internal motion in small silver clusters. The calculated dissociation energy was less satisfactory, while spin-polarization was found to be unimportant.

Ab initio MD simulations showed that the pattern of internal motion varied from Ag_4, to Ag_5 and Ag_6.

1. The rhombic and planar Ag_4 cluster are both stable at 200 K. At temperatures higher than 400 K, the planar structure isomerizes into the rhombic form. At 800 K, Ag_4 does not adopt a definite structure and the extent of internal motion is quite large.
2. In agreement with recent Raman measurement, the planar trapezoidal Ag_5 is the only stable isomer upon heating. At 800 K, the Ag_5 isomer maintained the planar structure, although atomic rearrangement does occur.
3. The most stable form for Ag_6 was the planar triangular structure. This structure was quite stable and rigid even at 800 K. The second most stable Ag_6 isomer, the pentagonal pyramid, was also stable up to 400 K. At 800 K, the pentagonal structure isomerizes into the planar trigonal structure.

We thank Mr. Frank Ng at the Computer Service Center of the Chinese University of Hong Kong for his help with the SGI Origin 2000, on which part of these simulations were performed. We also thank Dr. Doo Wan Boo at Department of Chemistry, University of Colorado at Boulder and Dr. Gong Xing Gao at The Institute of Solid State Physics, Chinese Academy of Sciences, Hefei, for their helpful discussions. This project was supported by an Earmarked Grant (Project No. CUHK 4188/97P) from the Research Grants Council of Hong Kong SAR Government.

References

1. W.A. de Heer, Rev. Mod. Phys. **65**, 611 (1993).
2. M. Brack, Rev. Mod. Phys. **65**, 677 (1993).
3. V. Bonačič-Koutecký, P. Fantucci, J. Koutecký, Chem. Rev. **91**, 1035 (1991).
4. R.S. Berry, T.L. Beck, H.L. Davis, J. Jellinek, Adv. Chem. Phys. **70**, 75 (1988).
5. A. Bulgac, D. Kusnezov, Phys. Rev. B **45**, 1988 (1992).
6. R. Car, M. Parrinello, Phys. Rev. Lett. **55**, 2471 (1985).
7. D.K. Remler, P.A. Madden, Mol. Phys. **70**, 921 (1990).
8. M.C. Payne, M.P. Teter, D.C. Allan, T.A. Arias, J.D. Joannopoulos, Rev. Mod. Phys. **64**, 1045 (1992).
9. G. Kresse, J. Hafner, Phys. Rev. B **47**, 558 (1993).
10. G. Kresse, J. Hafner, Phys. Rev. B **49**, 14251 (1991).
11. G. Kresse, J. Furthmüller, Comput. Mat. Sci. **6**, 15 (1996).
12. G. Kresse, J. Furthmüller, Phys. Rev. B **54**, 11169 (1996).
13. J. Jellinek, V. Bonăcić-Koutecký, P. Fantucci, M. Wiechert, J. Chem. Phys. **101**, 10092 (1994).
14. V. Bonačić-Koutecký, J. Jellinek, M. Wiechert, P. Fantucci, J. Chem. Phys. **107**, 6321 (1997).
15. U. Röthlisberger, W. Andreoni, J. Chem. Phys. **94**, 8129 (1991).
16. J.S. Tse, D.D. Klug, J. Chem. Phys. **101**, 473 (1994).
17. D.A. Gibson, E.A. Carter, Chem. Phys. Lett. **271**, 266 (1997).
18. T.L. Haslett, K.A. Bosnick, M. Moskovits, J. Chem. Phys. **108**, 3453 (1998).
19. J. Ho, K.M. Ervin, W.C. Lineberger, J. Chem. Phys. **93**, 6987 (1990).

20. H. Ruppe, S. Rutz, E. Schreiber, L. Wöste, Chem. Phys. Lett. **257**, 356 (1996).
21. S. Wolf, G. Sommerer, S. Rutz, E. Schreiber, T. Leisner, L. Wöste, R.S. Berry, Phys. Rev. Lett. **74**, 4177 (1995).
22. D.W. Boo, Y. Ozaki, L.H. Andersen, W.C. Lineberger, J. Phys. Chem. A **101**, 6686 (1997).
23. V. Beutel, G.L. Bhale, M. Kuhn, W. Demtröder, Chem. Phys. Lett. **185**, 313 (1991).
24. B. Simard, P.A. Hackett, A.M. James, P.R.R. Langridge-Smith, Chem. Phys. Lett. **186**, 415 (1991).
25. H.G. Krämer, V. Beutel, K. Weyers, W. Demtröder, Chem. Phys. Lett. **193**, 331 (1992).
26. K.J. Taylor, C.L. Pettiette-Hall, O. Cheshnovsky, R.E. Smalley, J. Chem. Phys. **96**, 3319 (1992).
27. S.B.H. Bach, D.A. Garland, R.J. van Zee, W. Weltner Jr, J. Chem. Phys. **87**, 869 (1987).
28. I. Rabin, W. Schulze, G. Ertl, J. Chem. Phys. **108**, 5137 (1998).
29. G. Alameddin, J. Hunter, D. Cameron, M.M. Kappe, Chem. Phys. Lett. **192**, 122 (1992).
30. H.O. Jeschke, M.E. Garcia, K.H. Bennemann, J. Phys. B: At. Mol. Opt. Phys. **29**, L545 (1996).
31. V. Bonačić-Koutecký, L. Češpiva, P. Fantucci, J. Koutecký, J. Chem. Phys. **98**, 7981 (1993).
32. V. Bonačić-Koutecký, L. Češpiva, P. Fantucci, J. Pittner, J. Koutecký, J. Chem. Phys. **100**, 490 (1994).
33. R. Poteau, J.L. Heully, F. Spiegelmann, Z. Phys. D **40**, 479 (1997).
34. R. Santamaria, I.G. Kaplan, O. Novaro, Chem. Phys. Lett. **218**, 395 (1994).
35. W. Andreoni, J.L. Martins, Surf. Sci. **156**, 635 (1985).
36. C.W. Bauschlicher Jr, S.R. Langhoff, P.R. Taylor, J. Chem. Phys. **88**, 1041 (1988).
37. C.W. Bauschlicher Jr, S.R. Langhoff, H. Partridge, J. Chem. Phys. **91**, 2412 (1989).
38. A. Ramírez-Solís, J.P. Daudey, O. Novaro, M.E. Ruíz, Z. Phys. D **15**, 71 (1990).
39. K. Balasubramanian, P.Y. Feng, Chem. Phys. Lett. **159**, 452 (1989).
40. C.W. Bauschlicher Jr, S.R. Langhoff, H. Partridge, J. Chem. Phys. **93**, 8133 (1990).
41. K. Balasubramanian, P.Y. Feng, J. Phys. Chem. **94**, 1536 (1990).
42. K.K. Das, K. Balasubramanian, Chem. Phys. Lett. **176**, 571 (1991).
43. D.W. Liao, K. Balasubramanian, J. Chem. Phys. **97**, 2548 (1992).
44. I.L. Garzón, I.G. Kaplan, R. Santamaria, O. Novaro, J. Chem. Phys. **109**, 2177 (1998).
45. I.L. Garzón, I.G. Kaplan, R. Santamaria, B.S. Vaisberg, O. Novaro, Z. Phys. D **40**, 202 (1997).
46. I.G. Kaplan, I.L. Gazón, R. Santamaria, B.S. Vaisberg, O. Novaro, Theo. Chem. **398-399**, 333 (1997).
47. B. Hartke, E.A. Carter, Chem. Phys. Lett. **216**, 324 (1993).
48. D.M. Ceperley, B.J. Alder, Phys. Rev. Lett. **45**, 566 (1980).
49. J.P. Perdew, in *Electronic Structure of Solids'91*, edited by P. Ziesche, H. Eschrig (Adademie Verlag, Berlin, 1991), p. 11.
50. G. Kresse, J. Hafner, J. Phys. Cond. Matt. **6**, 8245 (1994).
51. S. Nosé, J. Chem. Phys. **81**, 511 (1984).